UC Santa Barbara
UC Santa Barbara Previously Published Works

Title

Structure and optical band gaps of (Ba,Sr)SnO3 films grown by molecular beam epitaxy

Permalink

https://escholarship.org/uc/item/2s55w9g4

Journal

Journal of Vacuum Science & Technology A: Vacuum, Surfaces, and Films, 34(5)

ISSN

0734-2101 1520-8559

Authors

Schumann, Timo
Raghavan, Santosh
Ahadi, Kaveh
et al.

Publication Date

2016-09-01

DOI

10.1116/1.4959004

Peer reviewed

Structure and optical band gaps of (Ba,Sr)SnO3 films grown by molecular beam epitaxy

Timo Schumann, Santosh Raghavan, Kaveh Ahadi, Honggyu Kim, and Susanne Stemmer

LETTERS

Structure and optical band gaps of (Ba,Sr)SnO₃ films grown by molecular beam epitaxy

Timo Schumann,[a)] Santosh Raghavan,[a)] Kaveh Ahadi,[a)] Honggyu Kim, and Susanne Stemmer[b)]
Materials Department, University of California, Santa Barbara, California 93106-5050

Epitaxial growth of $(Ba_xSr_{1-x})SnO_3$ films with $0 \leq x \leq 1$ using molecular beam epitaxy is reported. It is shown that $SrSnO_3$ films can be grown coherently strained on closely lattice and symmetry matched $PrScO_3$ substrates. The evolution of the optical band gap as a function of composition is determined by spectroscopic ellipsometry. The direct band gap monotonously decreases with x from to 4.46 eV ($x = 0$) to 3.36 eV ($x = 1$). A large Burnstein-Moss shift is observed with La-doping of $BaSnO_3$ films. The shift corresponds approximately to the increase in Fermi level and is consistent with the low conduction band mass. © 2016 American Vacuum Society.
[http://dx.doi.org/10.1116/1.4959004]

Alkaline Earth stannates ($ASnO_3$ where A = Ca, Sr, or Ba) have attracted significant interest for use as transparent conductors[1,2] and as high-mobility, wide band gap channel materials in electronic devices,[3] where they can be integrated epitaxially with functional oxides that possess the same perovskite crystal structure. Room temperature electron mobilities in $BaSnO_3$ single crystals exceed 300 cm²/V s,[1] which is much higher than the carrier mobility of most perovskite oxides. For electronic devices, high-mobility epitaxial films with low defect concentrations and a range of band gaps are needed. The band gap and lattice parameters can be tuned by alloying $SrSnO_3$ and $BaSnO_3$,[4,5] thus presenting opportunities for the growth of lattice-matched films on different substrates, strain engineering, and tuning of heterojunction band offsets in this class of materials.

$BaSnO_3$ is cubic and has an indirect band gap, corresponding to transitions from the valence band maximum at the R point to the conduction band minimum at Γ.[6,7] A direct band gap is relatively close in energy.[6,7] $SrSnO_3$, which is orthorhombic (Pbnm space group[8]) is believed to either possess a direct gap (valence band maximum at Γ)[7] or the two band gaps are very close in energy.[9] The reported experimental band gap values for $BaSnO_3$ and $SrSnO_3$ range between 2.9 and 4.0 eV (Refs. 2, 7, and 10–13) and 4.1 eV to 4.27 eV,[7,10] respectively. Density functional theory (DFT) values also differ greatly.[6,13–16] Several factors affect the measured band gaps. Optical absorption is likely dominated by the direct band gap. For example, no significant changes in the optical absorption edge occur across the (Ba,Sr)SnO₃ series despite the presumed change in the nature of the band gap.[5] Doped samples[2] are expected to exhibit a large Burstein–Moss shift due to the small conduction band mass.[12,17,18] Recently, it

was suggested that doped samples also undergo a strong band gap renormalization.[19]

$BaSnO_3$ films have been grown by several techniques,[1,20–22] including molecular beam epitaxy (MBE),[19,23,24] which results in the highest mobility films,[24] whereas (Ba,Sr)SnO₃ and $SrSnO_3$ films have so far only been grown by high-energetic pulsed laser deposition.[19] Here, we demonstrate MBE of (Ba,Sr)SnO₃ and $SrSnO_3$ for systematic tuning of band gaps and film strain in epitaxial heterostructures.

$(Ba_xSr_{1-x})SnO_3$ films were grown using an MBE approach developed for $BaSnO_3$, where a SnO_2 source is used instead of elemental Sn, which addresses issues related to SnO volatility at low oxygen pressures typical in MBE.[24] SnO_2, Ba, Sr, and the La-dopant were supplied from effusion cells. Beam fluxes were calibrated using an ionization gauge and are given as beam equivalent pressure (BEP). Oxygen was provided by an RF-plasma source and the oxygen BEP was kept at 1.5×10^{-5} Torr. Prior to growth, the substrates were annealed at the growth temperature (800 °C, monitored via an optical pyrometer) under plasma exposure for 20 min. The SnO_x flux was set to a constant value of $\sim 1.5 \times 10^{-6}$ Torr, and the (Ba + Sr) flux to $\sim 5.0 \times 10^{-8}$ Torr. The (Ba + Sr)/SnO_x flux ratio was varied to optimize film stoichiometry. Unless stated otherwise, films were doped with La (0.2%–0.3%). Only the most Ba-rich films ($x = 1$ and $x = 0.8$) became electrically conductive when doped with La. The reason for the inability to dope Sr-rich films will be a subject of future investigations.

In situ reflection high-energy electron diffraction (RHEED) patterns were streaky throughout all growths, indicating smooth films. Post-growth characterization methods included high-resolution x-ray diffraction (XRD) with a Cu K^α x-ray source. The film thicknesses were determined from x-ray reflectivity. For (scanning) transmission electron microscopy (S/TEM) studies, cross-sectional samples were prepared by wedge polishing with a 2° angle and imaged using a field emission FEI Titan S/TEM operated at 300 keV. The

---

[a)]T. Schumann, S. Raghavan, and K. Ahadi contributed equally to this work.
[b)]Author to whom correspondence should be addressed; electronic mail: stemmer@mrl.ucsb.edu

direct band gap was analyzed using spectroscopy ellipsometry performed with a Wollam ellipsometer at incident angles of 60°–75° and photon energies from 0.7 to 6.5 eV.[25]

SrSnO₃ films were grown on (001) SrTiO₃ (lattice parameter $a = 3.905$ Å) and on closely lattice matched orthorhombic (110) PrScO₃ ($a_{pc} = 4.023$ Å, where the subscript indicates pseudocubic notation), which has the same space group as SrSnO₃ [$a_{pc} = 4.034$ Å (Ref. 8)]. The lattice mismatch between SrSnO₃ and PrScO₃ is thus very small, -0.27%. Out-of-plane high resolution XRD scans around the 002_{pc} reflections are shown in Fig. 1(a). Thickness fringes are much more pronounced for the film on PrScO₃, consistent with a coherently strained film and smoother interfaces/surfaces. (S)TEM images of the SrSnO₃ films are shown in Fig. 2. No misfit dislocations were detected in the film on PrScO₃, consistent with a coherently strained film, whereas the film on SrTiO₃ relaxes by incorporation of periodically spaced misfit dislocations.

Reciprocal space maps (RSM) around the 103_{pc} reflection were used to determine the in- and out-of-plane lattice parameters for all (Ba$_x$Sr$_{1-x}$)SnO₃ films. Examples are shown for SrSnO₃ in Figs. 1(c) and 1(d). On PrScO₃, the in-plane reciprocal lattice vectors of film and substrate align, indicating that the film is fully strained [Fig. 1(c)]. On SrTiO₃, the film is mostly relaxed, with a small residual compressive strain (-0.4%). The in-plane (a_{ip}) and out-of-plane (a_{oop}) lattice

parameters were used to calculate the unstrained film lattice parameter (a_0) as a function of composition[26]

$$a_0 = \frac{a_{oop} + 2\dfrac{c_{12}}{c_{11}}a_{ip}}{1 + 2\dfrac{c_{12}}{c_{11}}}, \qquad (1)$$

where c_{11} and c_{12} are the film elastic constants and c_{12}/c_{11} ~ 0.24.[27,28] a_0 is 4.041 ± 0.002 Å on PrScO₃ and 4.039 ± 0.006 Å on SrTiO₃, in close agreement with bulk SrSnO₃. Errors in a_0 (and thus also the errors for the composition in Fig. 3) were estimated from the standard deviation of two-dimensional Gaussian curves fitted to the diffraction peaks.

Out-of-plane x-ray diffraction scans of the 002 reflection of the Ba$_x$Sr$_{1-x}$SnO₃ alloys are shown in Fig. 1(b). The shifts to lower angles with increasing x (Ba content) are consistent with the expected increase in lattice parameter ($a_{BaSnO_3} = 4.116$ Å). The composition of the films was estimated by comparing a_0, determined as described above, with bulk values from the literature.[4]

Ellipsometry measurements of (Ba$_x$Sr$_{1-x}$)SnO₃ films were used to extract the optical absorption coefficient α.[25] Optical band gaps were then estimated from Tauc plots, i.e., the relation[29]
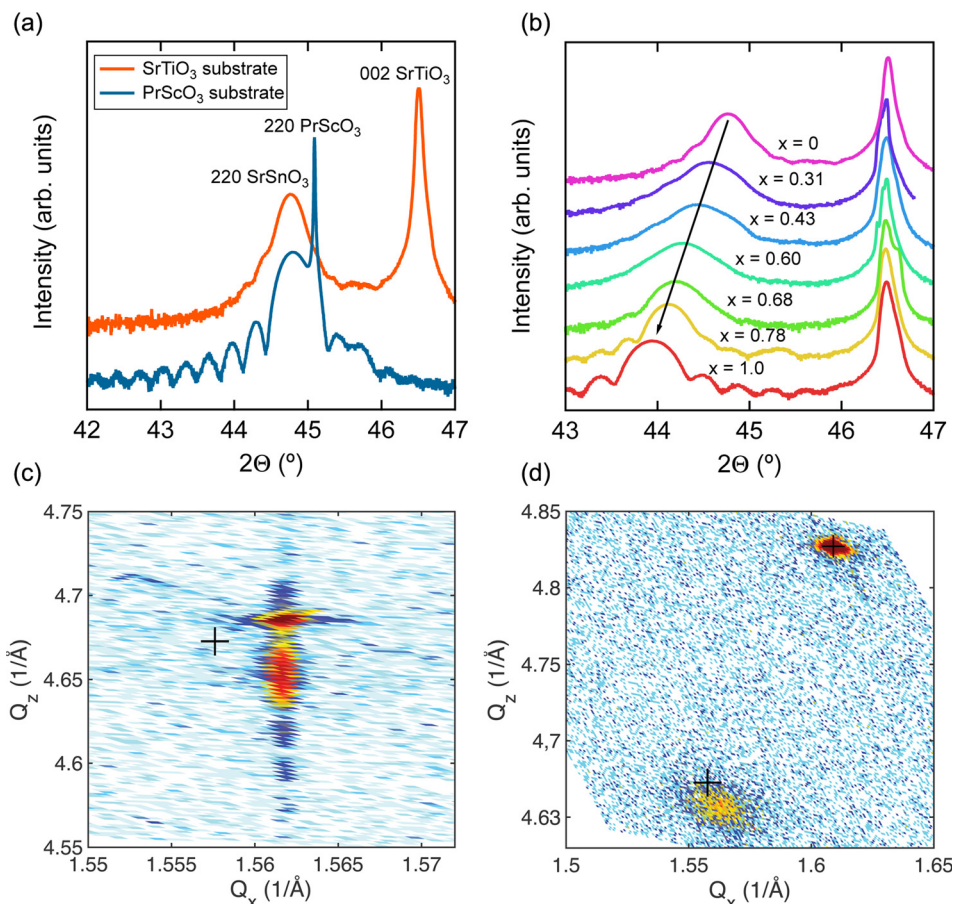
FIG. 1. (Color online) (a) Out-of-plane XRD of SrSnO₃ films on SrTiO₃ (film thickness ~41 nm) and PrScO₃ (film thickness ~31 nm), respectively. (b) Out-of-plane XRD of Ba$_x$Sr$_{1-x}$O₃ films. The film thicknesses range between 25 and 41 nm. (c) RSM around the 103_{pc} reflection for a SrSnO₃ film on PrScO₃. (d) Same as (c) except for a film on a SrTiO₃ substrate. The axes denote the in-plane (Q_x) and out-of-plane (Q_z) scattering vectors, scaled as $2\pi/a$, where a is the real-space distance of the respective lattice plane. The black crosses indicate the expected values for relaxed, bulk SrSnO₃.

FIG. 2. (a) and (b) Dark-field TEM image and high-angle annular dark-field (HAADF)-STEM image of a SrSnO₃ film grown on SrTiO₃. The white arrows i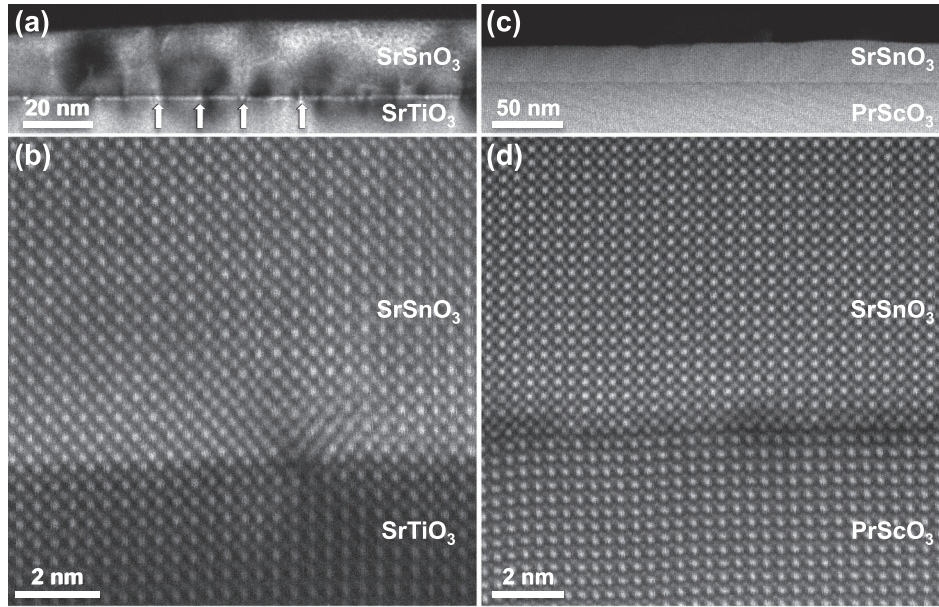n (a) indicate the location of misfit dislocations at the interface. (c) and (d) HAADF-STEM images of SrSnO₃ films grown on PrScO₃, showing epitaxial growth and no detectable extended defects.

$$(h\upsilon\alpha)^n = A(h\upsilon - E_g), \qquad (2)$$

where h is Planck's constant, A a constant, υ is the frequency, E_g the band gap, and n a constant that indicates the nature of the transition (i.e., direct/indirect, allowed/forbidden). Here, we use $n = 2$, corresponding to a direct allowed band gap. Although undoped BaSnO₃ could also be fit to an indirect model ($n = 0.5$), similar to Ref. 11, the absorption is orders of magnitude too high for a typical indirect band gap in a thin film.[30] Therefore, only the direct band gap should be extracted. Tauc plots for differently doped BaSnO₃ films and for SrSnO₃ are shown in Fig. 3(a). Figure 3(b) shows the extracted band gap values for all compositions. The band gap monotonously increases with decreasing x but does not follow a linear Vegard's law. Since the films on SrTiO₃ are (almost) completely relaxed, we expect no large strain effects on the measured band gaps. The measured band gap values can be compared with those reported in the literature; most data are for BaSnO₃. The measured band gap (3.36 eV) for the undoped MBE BaSnO₃ film is somewhat smaller than values reported for single crystals from ellipsometry ($\sim$3.5 eV),[13] thin films in ellipsometry and optical absorption,[10,11] and slightly larger than that of ceramics and single crystals characterized by optical absorption ($\sim$3.1 eV).[7,12]

Doping increases the measured optical band gap (Fig. 3), due to a pronounced Burstein–Moss shift, which is due to the increase in Fermi level. For a single, parabolic conduction band minimum, which is a good approximation for BaSnO₃, the position of the Fermi level (E_F) above the conduction band minimum (E_{CBM}) is given by

$$(E_F - E_{CBM}) = \frac{h^2}{8m^*}\left(\frac{3}{\pi}\right)^{2/3} n_{3D}^{2/3}, \qquad (3)$$
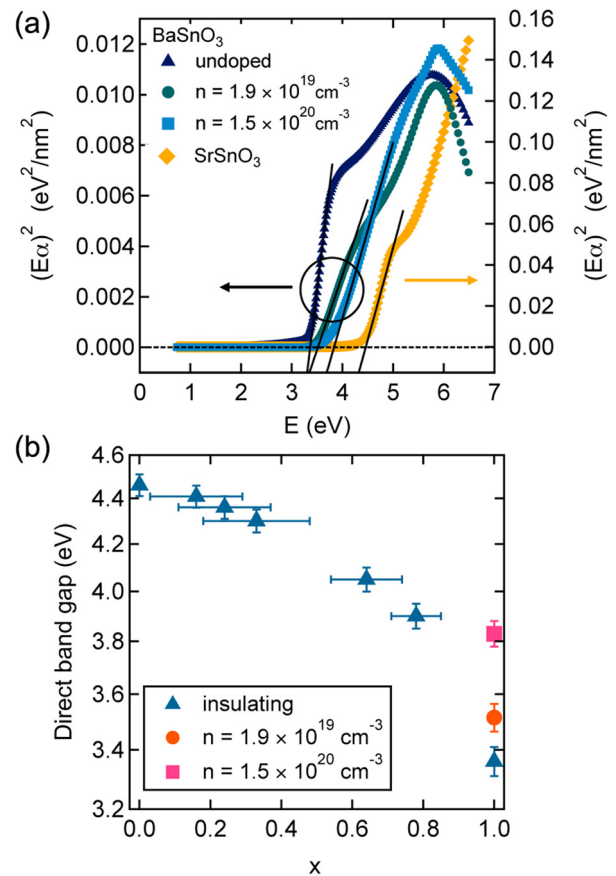
FIG. 3. (Color online) (a) Plots of $(E\alpha)^2$ as a function of photon energy E, which were used to determine the band gaps from spectroscopic ellipsometry, shown here for SrSnO₃ and BaSnO₃ with three different carrier densities: nominally undoped, $n_{3D} = 2.9 \times 10^{19}\,\text{cm}^{-3}$ and $1.5 \times 10^{20}\,\text{cm}^{-3}$. (b) Extracted band gap values for Ba$_x$Sr$_{1-x}$SnO₃ films, with x determined from the lattice parameter measurements.

where $m*$ is the effective mass ($\sim$0.19 m_0,[18] m_0 is the free electron mass) and n_{3D} is the carrier density. For the two doping densities $n_{3D} = 2.9 \times 10^{19}$ and 1.5×10^{20} cm^{-3}, $E_F - E_{CBM}$ is 0.18 and 0.55 eV, respectively. The fraction of ionized dopants was previously estimated to be $\sim$90%.[18] These values are in close agreement with the increase in the optical band gap for these two samples, of 0.15 and 0.47 eV, respectively, relative to the undoped sample (see Fig. 3). In Ref. 19, a band gap renormalization (shrinking) of $\sim$0.4 eV is suggested for a sample doped to $\sim$10^{20} cm^{-3}, which should have almost completely eliminated the Burstein–Moss shift. Thus the data reported here do not support a strong band gap normalization. This experimental result is also consistent with predictions from DFT.[17]

In summary, high-quality, MBE grown (Ba$_x$Sr$_{1-x}$)SnO$_3$ films allow for developing band gap and strain engineered heterostructures with the perovskite stannates. They also provide a consistent picture of the relationship between their composition and optical properties. In particular, the band gap measurements of doped BaSnO$_3$ films are consistent with the light conduction band mass resulting in a strong Burstein–Moss shift, but only a small band gap renormalization. The much improved structural quality of SrSnO$_3$ films on a nearly lattice matched substrate, PrScO$_3$, as evidenced by XRD and TEM, augurs well for future improvements in mobility for BaSnO$_3$, if more closely lattice matched substrates that allow for similar reductions in extended defect densities, could be obtained.

ACKNOWLEDGMENTS

[1]H. J. Kim *et al.*, Appl. Phys. Express **5**, 061102 (2012).

[2]X. Luo, Y. S. Oh, A. Sirenko, P. Gao, T. A. Tyson, K. Char, and S. W. Cheong, Appl. Phys. Lett. **100**, 172112 (2012).

[3]S. Ismail-Beigi, F. J. Walker, S. W. Cheong, K. M. Rabe, and C. H. Ahn, APL Mater. **3**, 062510 (2015).

[4]E. H. Mountstevens, J. P. Attfield, and S. A. T. Redfern, J. Phys. Condens. Mater. **15**, 8315 (2003).

[5]H. Mizoguchi, P. M. Woodward, C. H. Park, and D. A. Keszler, J. Am. Chem. Soc. **126**, 9796 (2004).

[6]D. J. Singh, D. A. Papaconstantopoulos, J. P. Julien, and F. Cyrot-Lackmann, Phys. Rev. B **44**, 9519 (1991).

[7]H. Mizoguchi, H. W. Eng, and P. M. Woodward, Inorg. Chem. **43**, 1667 (2004).

[8]A. Vegas, M. Vallet-Regi, J. M. Gonzalez-Calbet, and M. A. Alario-Franco, Acta Cryst. B **42**, 167 (1986).

[9]K. P. Ong, X. Fan, A. Subedi, M. B. Sullivan, and D. J. Singh, APL Mater. **3**, 062505 (2015).

[10]Q. Liu, *et al.*, EPL **98**, 47010 (2012).

[11]S. A. Chambers, T. C. Kaspar, A. Prakash, G. Haugstad, and B. Jalan, Appl. Phys. Lett. **108**, 152104 (2016).

[12]H. J. Kim *et al.*, Phys. Rev. B **86**, 165205 (2012).

[13]T. N. Stanislavchuk, A. A. Sirenko, A. P. Litvinchuk, X. Luo, and S.-W. Cheong, J. Appl. Phys. **112**, 044108 (2012).

[14]D. O. Scanlon, Phys. Rev. B **87**, 161201(R) (2013).

[15]L. Bjaalie, B. Himmetoglu, L. Weston, A. Janotti, and C. G. Van de Walle, New J. Phys. **16**, 025005 (2014).

[16]H.-R. Liu, J.-H. Yang, H. J. Xiang, X. G. Gong, and S.-H. Wei, Appl. Phys. Lett. **102**, 112109 (2013).

[17]Y. Li, L. Zhang, Y. Ma, and D. J. Singh, APL Mater. **3**, 011102 (2015).

[18]S. J. Allen, S. Raghavan, T. Schumann, K.-M. Law, and S. Stemmer, Appl. Phys. Lett. **108**, 252107 (2016).

[19]Z. Lebens-Higgins *et al.*, Phys. Rev. Lett. **116**, 027602 (2016).

[20]K. Ganguly, P. Ambwani, P. Xu, J. S. Jeong, K. A. Mkhoyan, C. Leighton, and B. Jalan, APL Mater. **3**, 062509 (2015).

[21]P. V. Wadekar *et al.*, Appl. Phys. Lett. **105**, 052104 (2014).

[22]W.-J. Lee *et al.*, Appl. Phys. Lett. **108**, 082105 (2016).

[23]A. Prakash, J. Dewey, H. Yun, J. S. Jeong, K. A. Mkhoyan, and B. Jalan, J. Vac. Sci. Technol., A **33**, 060608 (2015).

[24]S. Raghavan, T. Schumann, H. Kim, J. Y. Zhang, T. A. Cain, and S. Stemmer, APL Mater. **4**, 016106 (2016).

[25]See supplementary material at http://dx.doi.org/10.1116/1.4959004 for details of the ellipsometry measurements and additional x-ray scans.

[26]B. Bauer and W. Richter, *Optical Characterization of Epitaxial Semiconductor Layers* (Springer, Berlin, 1996).

[27]I. R. Shein, V. L. Kozhevnikov, and A. Ivanovskii, Solid State Sci. **10**, 217 (2008).

[28]B. Ghebouli, M. A. Ghebouli, T. Chihi, M. Fatmi, S. Boucetta, and M. Reffas, Solid State Commun. **149**, 2244 (2009).

[29]J. Tauc, R. Grigorov, and A. Vancu, Phys. Status Solidi **15**, 627 (1966).

[30]A. Ghosh, C. M. Nelson, L. S. Abdallah, and S. Zollner, J. Vac. Sci. Technol. A **33**, 061203 (2015).